

REPORT DOCUMENTATION PAGE					<i>Form Approved</i> OMB No. 0704-0188	
The public reporting burden for this collection of information is estimated to average 1 hour per response, including the time for reviewing instructions, searching existing data sources, gathering and maintaining the data needed, and completing and reviewing the collection of information. Send comments regarding this burden estimate or any other aspect of this collection of information, including suggestions for reducing the burden, to Department of Defense, Washington Headquarters Services, Directorate for Information Operations and Reports (0704-0188), 1215 Jefferson Davis Highway, Suite 1204, Arlington, VA 22202-4302. Respondents should be aware that notwithstanding any other provision of law, no person shall be subject to any penalty for failing to comply with a collection of information if it does not display a currently valid OMB control number. PLEASE DO NOT RETURN YOUR FORM TO THE ABOVE ADDRESS.						
1. REPORT DATE (DD-MM-YYYY) 09-06-2014		2. REPORT TYPE Final		3. DATES COVERED (From - To) 7 Mar 2012 to 7 Mar 2014		
4. TITLE AND SUBTITLE Fabrication of Porous Carbon-based Nanostructure for Energy Storage and Transfer Applications				5a. CONTRACT NUMBER FA23861214033		
				5b. GRANT NUMBER		
				5c. PROGRAM ELEMENT NUMBER		
6. AUTHOR(S) Prof Kian Ping Loh				5d. PROJECT NUMBER		
				5e. TASK NUMBER		
				5f. WORK UNIT NUMBER		
7. PERFORMING ORGANIZATION NAME(S) AND ADDRESS(ES) National University of Singapore 3 Science Drive 3 Singapore 117546 Singapore				8. PERFORMING ORGANIZATION REPORT NUMBER N/A		
9. SPONSORING/MONITORING AGENCY NAME(S) AND ADDRESS(ES) AOARD UNIT 45002 APO AP 96338-5002				10. SPONSOR/MONITOR'S ACRONYM(S) AOARD		
				11. SPONSOR/MONITOR'S REPORT NUMBER(S) AOARD-124033		
12. DISTRIBUTION/AVAILABILITY STATEMENT Approved for public release.						
13. SUPPLEMENTARY NOTES						
14. ABSTRACT We have demonstrated a method to improve the capacity of microporous graphene electrodes by in-filling its cavities with graphene eggshells. The eggshell increases the volumetric energy density and its interconnected networks shorten the Li-ion diffusion pathway and ultimately enhance the rate capabilities. Such morphology control is also effective in improving the initial coulombic efficiency of the unfilled graphene foam by 17%. Mechanistic study using <i>in-situ</i> Raman and <i>ex-situ</i> NMR reveals that the Li intercalation mechanism of GE@GF electrode resembles that of bulk graphite, that is, <i>via</i> stage Li-graphite intercalated compounds, although its overall capacity is higher than that of the theoretical values of graphite.						
15. SUBJECT TERMS Energy Conversion, Energy Storage System, nanostructures, Graphene						
16. SECURITY CLASSIFICATION OF:			17. LIMITATION OF ABSTRACT	18. NUMBER OF PAGES	19a. NAME OF RESPONSIBLE PERSON	
a. REPORT	b. ABSTRACT	c. THIS PAGE			Tammy Low, Lt Col, USAF, Ph.D.	
U	U	U	UU	15	19b. TELEPHONE NUMBER (Include area code) +81-3-5410-4409	

Report Documentation Page			Form Approved OMB No. 0704-0188		
Public reporting burden for the collection of information is estimated to average 1 hour per response, including the time for reviewing instructions, searching existing data sources, gathering and maintaining the data needed, and completing and reviewing the collection of information. Send comments regarding this burden estimate or any other aspect of this collection of information, including suggestions for reducing this burden, to Washington Headquarters Services, Directorate for Information Operations and Reports, 1215 Jefferson Davis Highway, Suite 1204, Arlington VA 22202-4302. Respondents should be aware that notwithstanding any other provision of law, no person shall be subject to a penalty for failing to comply with a collection of information if it does not display a currently valid OMB control number.					
1. REPORT DATE 09 JUN 2014		2. REPORT TYPE Final		3. DATES COVERED 07-03-2012 to 07-03-2014	
4. TITLE AND SUBTITLE Fabrication of Porous Carbon-based Nanostructure for Energy			5a. CONTRACT NUMBER FA23861214033		
			5b. GRANT NUMBER		
			5c. PROGRAM ELEMENT NUMBER		
6. AUTHOR(S) Kian Ping Loh			5d. PROJECT NUMBER		
			5e. TASK NUMBER		
			5f. WORK UNIT NUMBER		
7. PERFORMING ORGANIZATION NAME(S) AND ADDRESS(ES) National University of Singapore,3 Science Drive 3,Singapore 117546,Singapore,NA,NA			8. PERFORMING ORGANIZATION REPORT NUMBER N/A		
9. SPONSORING/MONITORING AGENCY NAME(S) AND ADDRESS(ES) AOARD, UNIT 45002, APO, AP, 96338-5002			10. SPONSOR/MONITOR'S ACRONYM(S) AOARD		
			11. SPONSOR/MONITOR'S REPORT NUMBER(S) AOARD-124033		
12. DISTRIBUTION/AVAILABILITY STATEMENT Approved for public release; distribution unlimited					
13. SUPPLEMENTARY NOTES					
14. ABSTRACT We have demonstrated a method to improve the capacity of microporous graphene electrodes by in-filling its cavities with graphene eggshells. The eggshell increases the volumetric energy density and its interconnected networks shorten the Li-ion diffusion pathway and ultimately enhance the rate capabilities. Such morphology control is also effective in improving the initial coulombic efficiency of the unfilled graphene foam by 17%. Mechanistic study using in-situ Raman and ex-situ NMR reveals that the Li intercalation mechanism of GE@GF electrode resembles that of bulk graphite, that is, via stage Li-graphite intercalated compounds, although its overall capacity is higher than that of the theoretical values of graphite.					
15. SUBJECT TERMS Energy Conversion, Energy Storage System, nanostructures, Graphene					
16. SECURITY CLASSIFICATION OF:			17. LIMITATION OF ABSTRACT Same as Report (SAR)	18. NUMBER OF PAGES 15	19a. NAME OF RESPONSIBLE PERSON
a. REPORT unclassified	b. ABSTRACT unclassified	c. THIS PAGE unclassified			

Fabrication of Porous Carbon-based nanostructure for Energy Storage and Transfer Applications

Name of Principal Investigators (PI and Co-PIs): KIAN PING LOH

- e-mail address : chmlohkp@nus.edu.sg
- Institution : National University of Singapore
- Mailing Address : 3 Science Drive 3, Singapore 117543
- Phone : 96207002
- Fax : 67791691

Period of Performance: MARCH/7/2012 – MARCH/07/2014

1. Introduction

The current lithium ion batteries (LIB) are considered to be one of the most practical solutions to the rapidly growing demand for energy.¹⁻³ Large-scale energy applications in electric grids, defence, aerospace, transportation and small portable devices drive the demand for high-performance electrode materials with the capability to store and deliver more energy efficiently.⁴ The electrode reaction in a rechargeable lithium battery relies on the simultaneous intercalation of Li^+ and e^- into the active intercalation host.⁵ While the shape of the voltage profile and the intrinsic storage capacity are determined by thermodynamic properties of the intercalation host, the rate with which a lithium battery can be charged and discharged depends on kinetic properties like Li ion mobility and phase transformation mechanism. In the conventional intercalation compounds, the self-diffusion coefficient (D) of Li ion described by the Einstein-Smoluchowski diffusion equation is expressed as follows⁶:

$$D = \frac{\lambda^2 k_B T}{4h} \exp\left(-\frac{\Delta E_{\text{diff}}}{k_B T}\right)$$

(1)

where h , k_B and T are Planck's constant, Boltzmann constant and temperature, respectively; λ and E_{diff} , denote the diffusion length and diffusion barrier of Li^+ in intercalation compound based on transition state theory.⁷ Any variation of the chemical diffusion coefficient D with Li concentration therefore arises from a dependence of the diffusion barrier and vibrational prefactors on the average Li concentration. Due to the exponential dependence of D on ΔE_{diff} , a small variation in the diffusion barrier due to compositional, chemical or crystallographic changes translates into a large change in the diffusion coefficient, especially at room temperature. As such, there is a need for nanostructured material that can support fast lithium diffusion and accommodate the strain associated with lithium intercalation.^{8,9}

Carbonaceous materials, especially graphite, are the most widely employed negative electrode for commercial lithium batteries on account of its low cost, long lifespan, non-toxicity and high safety record.^{10,11} However, the theoretical capacity of graphite is only 372 mAh/g. Strategies used to boost the power capability of electrode materials for Li-ion batteries generally involve reducing the domain size of the active charge-storage material in the electrode to shorten the ion diffusion paths. Nanostructures are particularly attractive in providing fast kinetics.¹² Graphene, as the fundamental building blocks of graphite, has been widely used in energy-related applications.^{13,14} It has been touted as possible candidates to improve the performance of LIB due to its high surface area, extraordinary in-plane electrical conductivity, excellent tensile modulus and mechanical durability.^{15, 16} When rendered in the nanoporous form like graphene foam, the high surface area and free

space may buffer the volume swing that occur during charge/discharge cycling of embedded high-capacity metals or metal oxide materials, thereby minimizing electrode destruction from the associated strain.^{12,17} Previous work by Ji *et al*¹⁸ and Li *et al*¹⁹ have demonstrated that graphene foam impregnated with anode material ($\text{Li}_4\text{Ti}_5\text{O}_{12}$) and cathode material (lithium iron phosphate and LiFePO_4) shows high rate capability in LIB. On its own, such foam-like material is known to have low volumetric energy density, thus a material synthesis strategy which allows porosity and yet maintaining high volumetric energy density is needed.

In this work, we develop a porous network composed of hollow graphene “eggshells” filling three-dimensional (3D) graphene foam. In theory, such a unique carbon nanostructure is expected to manifest greatly improved electrochemical performance because of the integration of several advantageous structure features. First, it can offer a high density of cross-plane ion diffusion channels that facilitate charge transport. Second, it can be better for lithium intercalation at high rates due to the strained hollow egg shell structure. Under biaxial asymmetric strain, it has been calculated that the binding energy of Li to graphene sheet increases by 52% with respect to its bulk's cohesive energy.²⁰ Third, the hollow structure provides sufficient buffering for volume swing during lithiation and delithiation. At the same time, its multichannels allows fast ionic transport through the electrode during cycling.^{21,22} Finally, the in-filling of the 3D graphene foam by the graphene egg shells enhances the volumetric density, electrochemical activity and mechanical stability.²³

2. Experimental Section

The as-synthesized GF and GE@GF electrodes were cut into 16 mm diameter electrodes and dried in oven at 80°C. The cells were assembled in an argon-filled glove box with metallic lithium (thickness, Kyokuto metal Co, Japan,) as the reference and counter electrode, 1M LiPF₆ in ethylene carbonate (EC)-dimethyl carbonate (DMC) (1:1 volume ratio) as the electrolyte and a polypropylene (PP) micro-porous film (Whatman) as the separator. Galvanostatic charge-discharge cycling was carried out on a Bitrode battery tester system (Model SCN-12-4-5/18, USA) in the voltage range of 3.0 to 0.005 V (versus Li/Li⁺). Cyclic voltammetry (CV) was performed on a computer controlled MacPile II unit (Biological, France) at room temperature at a scan rate of 0.058 mVs⁻¹ from 0.005 to 3.0 V. Details of electrode fabrication and instrumentation were presented in previous report.^{24, 25}

3. Results and discussion

The synthesis strategy of graphene eggshell-filled graphene foam (denoted as GE@GF) is based on a conventional chemical impregnation method for the preparation of catalyst, followed by chemical vapor deposition (CVD) growth of graphene film and then chemical etching of metal catalyst, as schematically illustrated in Figure 1a (Details in supporting information). Briefly, an appropriate slurry in viscosity was prepared by mixing Ni powder (2.2 ~3 μm in diameter) and poly (methyl methacrylate) PMMA (950 PMMA A5, 5% in anisole) under sonication for 30 min. The resulting slurry was well homogenized and was slowly drop-casted

into nickel foams (Alantum Advanced Technology Materials (Dalian), $\sim 380\text{g/m}^2$ in area density and $\sim 1.2\text{mm}$ in thickness). The as-prepared PMMA-coated Ni-powder@Ni foam was baked at $80\text{ }^\circ\text{C}$ for 5h and then annealed at $200\text{ }^\circ\text{C}$ for 10h. After this, Ni-powder@Ni foam samples were introduced into the furnace for the CVD growth of graphene, where PMMA plays two roles: (1) fixing the Ni powder in Ni foam and (2) provides solid carbon source for the growth of graphene.²⁶ Figure 1h shows the novel graphene hybrid nanostructure at different stage from Ni foam (i) to Ni-powder@Ni foam (ii) and the one after CVD growth (iii).

In Figure 1b, it can be seen that the Ni foam exhibits a microporous structure with pore sizes ranging from 100 to 400 μm as imaged by Field-emission Scanning Electron Microscopy (FESEM). After the etching of the Ni foam, the recovered 3D graphene foam shows comparable pore sizes, as shown in Figure 1c. By introducing graphene eggshells into the pores of the graphene foam, the density and mechanical strength of the whole hybrid system was dramatically increased, as shown in Figures 1d and 1e. As shown, the graphene eggshells are packed tightly within the graphene foam (Figure S1), which gives an interconnected electrically conducting network. Meanwhile, the cavity in each graphene eggshell can store Li ions (Figures 1f and 1g). Energy dispersive X-ray (EDX) analysis (Figure 1i) confirmed the complete removal of Ni powder and Ni foam after the chemical etching. The hybrid GE@GF nanostructure was also characterized by Raman spectroscopy (514 nm excitation). Figure 1j show two distinct peaks at $\sim 1580\text{ cm}^{-1}$ (G-band) and 2705 cm^{-1} (2D-band). One commonly used parameter for judging the layer thickness is the 2D band at 2700 cm^{-1} , which is an overtone of the disorder-induced D band located at 1350 cm^{-1} .²⁷ The 2D band in monolayer G can be fitted to a single Lorentzian peak

and its full width at half-maximum (FWHM) is $\sim 30 \text{ cm}^{-1}$, whereas bilayer G can be fitted with four Lorentzian components.²⁸ With the increase of layer number, the 2D band evolves into a two-peak structure along with a concomitant decrease in intensity with respect to the G band ($\sim 1580 \text{ cm}^{-1}$). On the basis of Raman peak profile analysis, the hybrid GE@GF consists of few-layer graphene (Figure S2).

The detailed structure of GE@GF is further elucidated by high-resolution transmission electron microscopy (HR-TEM) and selected-area electron diffraction (SAED). In agreement with the above SEM findings, a well-defined cavity can be observed inside each microsphere (Figures 2a and 2c). Figure 2b shows a HRTEM image of the graphene eggshell, where the $\{002\}$ lattice fringes (3.4 \AA) can be clearly observed. The SAED pattern suggests the graphene eggshells are polycrystalline.

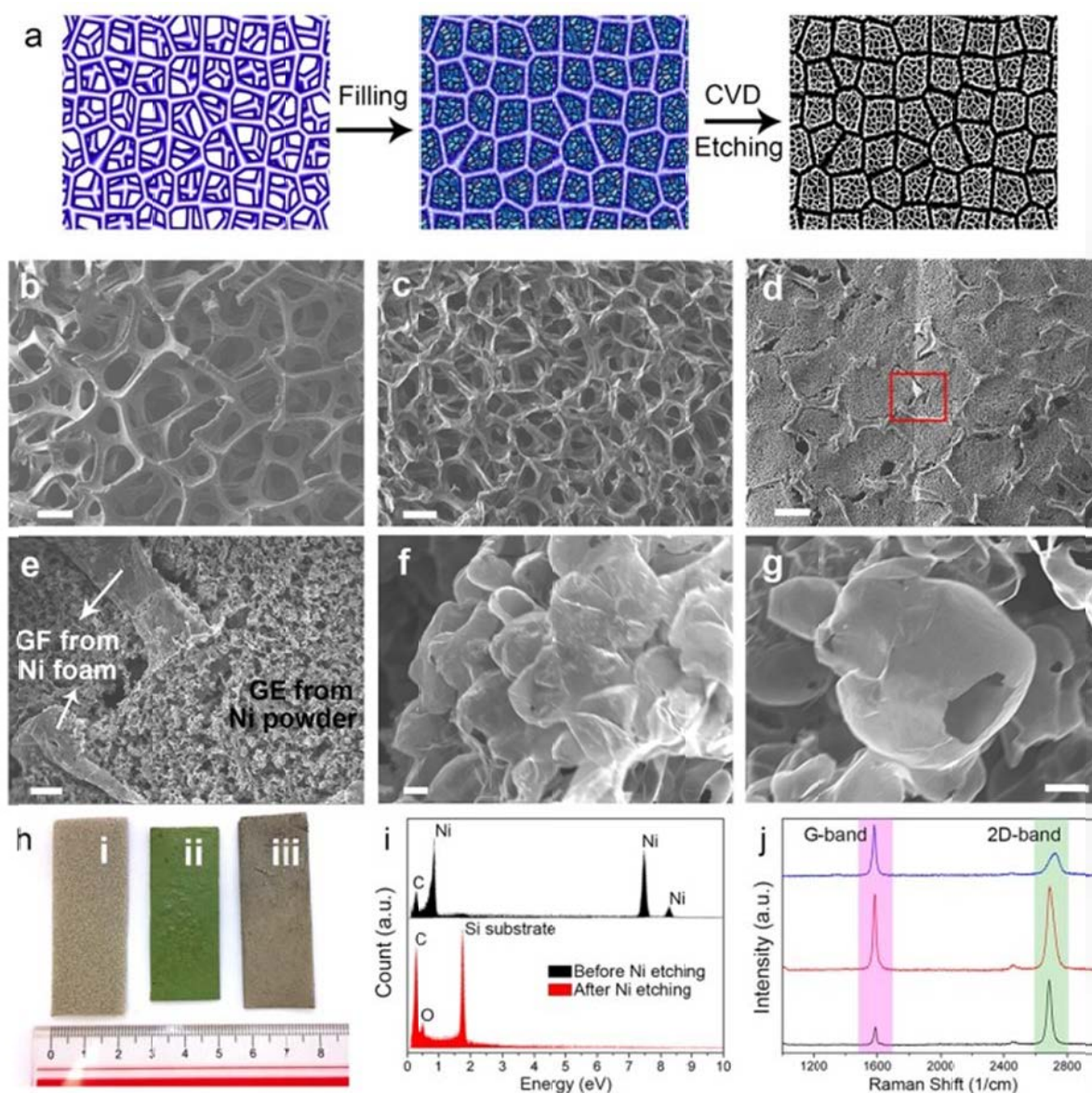


Figure 1. (a) Schematic illustration of the graphene eggshell-filled graphene foam (GE@GF); (b), (c) SEM images of graphene foam before and after Ni etching (scale bar = 200 μm). (d) A typical low-magnification SEM image of the GE@GF structure (scale bar = 200 μm). (e) A magnified SEM image of the red square in (d) (scale bar = 20 μm). (f), (g) graphene eggshell structure with open cavities (scale bar = 1 μm). (h) Optical image of the hybrid structure at the different stages. (i) Ni foam; (ii) and (iii) As-prepared Ni-powder@Ni foam before and after CVD growth, respectively. (i) Comparison of EDX spectra before and after Ni etching. (j) Raman measurements.

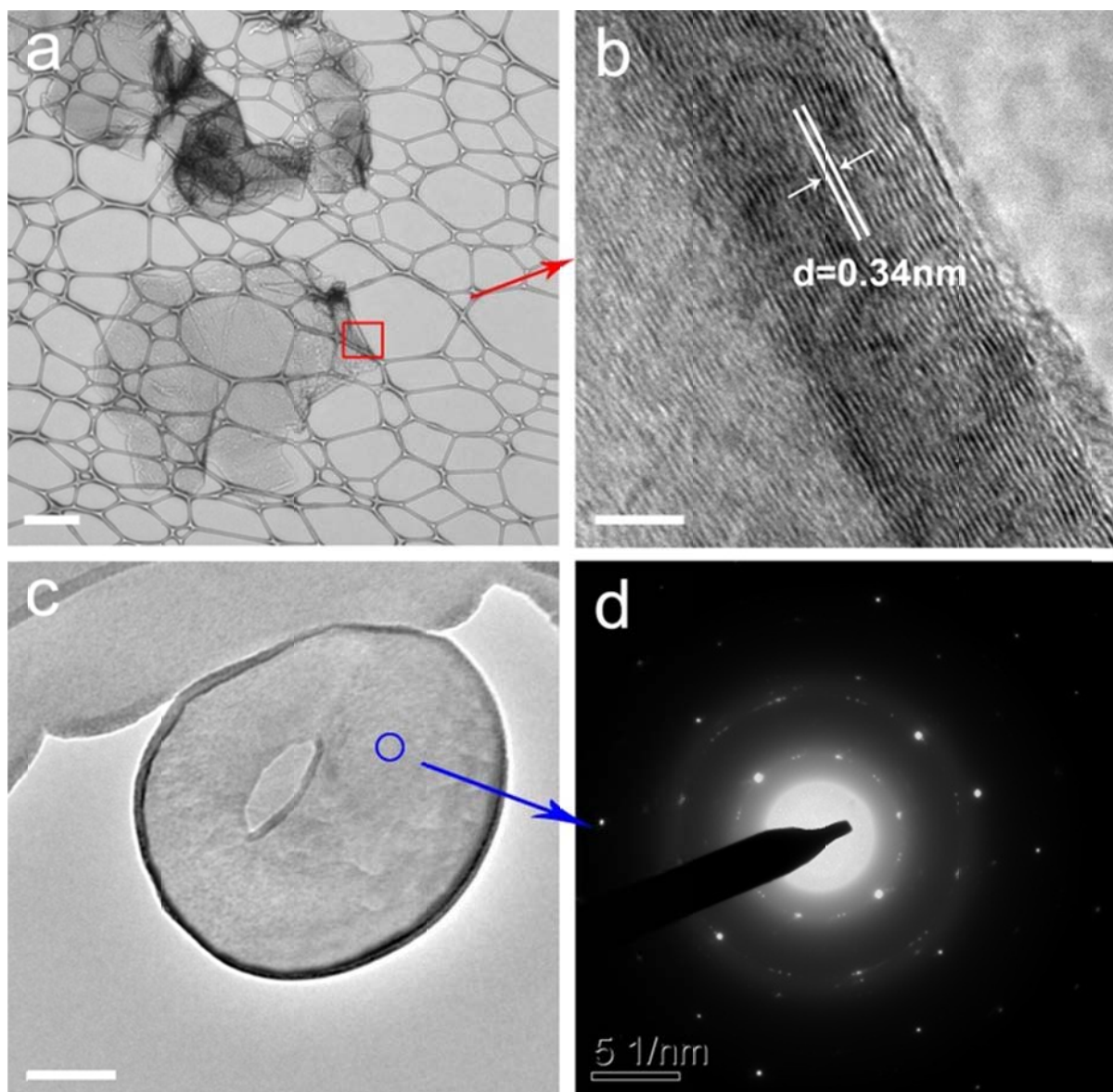


Figure 2. (a), (c) TEM images of graphene egg shell structure (scale bar = 500 nm). (b) HRTEM image of the red square in (a), showing crystalline shell wall (scale bar = 2 nm). (d) SAED pattern of the shell wall at the blue circle in (c).

Potato-shaped graphite has been reported to have reduced irreversible capacity and high rate performance,²⁹ hence we like to find out if the hollow graphene eggshell could achieve the same objectives. Both GF and GE@GF electrodes are subjected to galvanostatic cycling at low current rate of 37 mA g^{-1} in a 1M LiPF_6 electrolyte. The

electrochemical performances of the GF and GE@GF are shown in Figure 3. Overall, the cycling profiles of both electrodes resembles that of graphite.³⁰ During discharge cycle (intercalation), both materials showed a plateau at $\sim 0.75\text{V}$ vs. Li/Li^+ ; this is due to the solid electrolyte interface (SEI) caused by the electrolyte decomposition. Another major plateau is observed at $\sim 0.20\text{V}$ which corresponds to Li intercalation. GF electrode delivers the first discharge and reversible capacity at 557 and $370 (\pm 5)$ mAh g^{-1} , respectively. After 45 cycles, the capacity reaches 366 mAh g^{-1} (Figure 3a). For GE@GF electrode, the first discharge capacity is 424 mAh g^{-1} , while the reversible capacity achieves 328 mAh g^{-1} . Upon reaching 45 cycles, the capacity increases to 368 mAh g^{-1} which is comparable to GF electrode (Figure 3b). There are some differences in the galvanostatic curves after the first cycle. At 0.2V , the GE electrode exhibits flat plateau whereas a hysteretic profile is more prominent for GE@GF electrode. This non-flat plateau suggests the pseudocapacitive storage behaviour of the electrode.¹⁹

The Li storage mechanism of both electrodes can also be studied carefully by slow scanning cyclic voltammetry. Voltammograms of GF and GE@GF in Figures 3c and 3d depict the reversibility of Li intercalation and deintercalation. The broader curve of GE@GF further reveals capacitive behaviour which may be attributed to the interfacial storage of Li on hollow graphene eggshell.

Figures 3e and 3f show the cycling stability of both electrodes. It is noted that the initial coulombic efficiency increases from 66.3% for GF to 77.5% for GE@GF electrode. This suggests that the in-filling of the foam by the graphene eggshell reduces the electrolyte decomposition and surface side reaction. The gradual increase in the capacity of GE@GF electrode upon cycling may be attributed to the

interconnected graphene eggshell which enhances the ionic diffusion throughout the graphene network. In addition, with cycling, increasing number of active sites and surface defects on the hollow graphene eggshell are activated for Li accommodation. Hence, we surmise that the curvature in the hollow graphene eggshell alters the λ and E_{diff} of Li ion, and provides a more efficient intercalation/ deintercalation pathway and reduces the initial capacity loss.

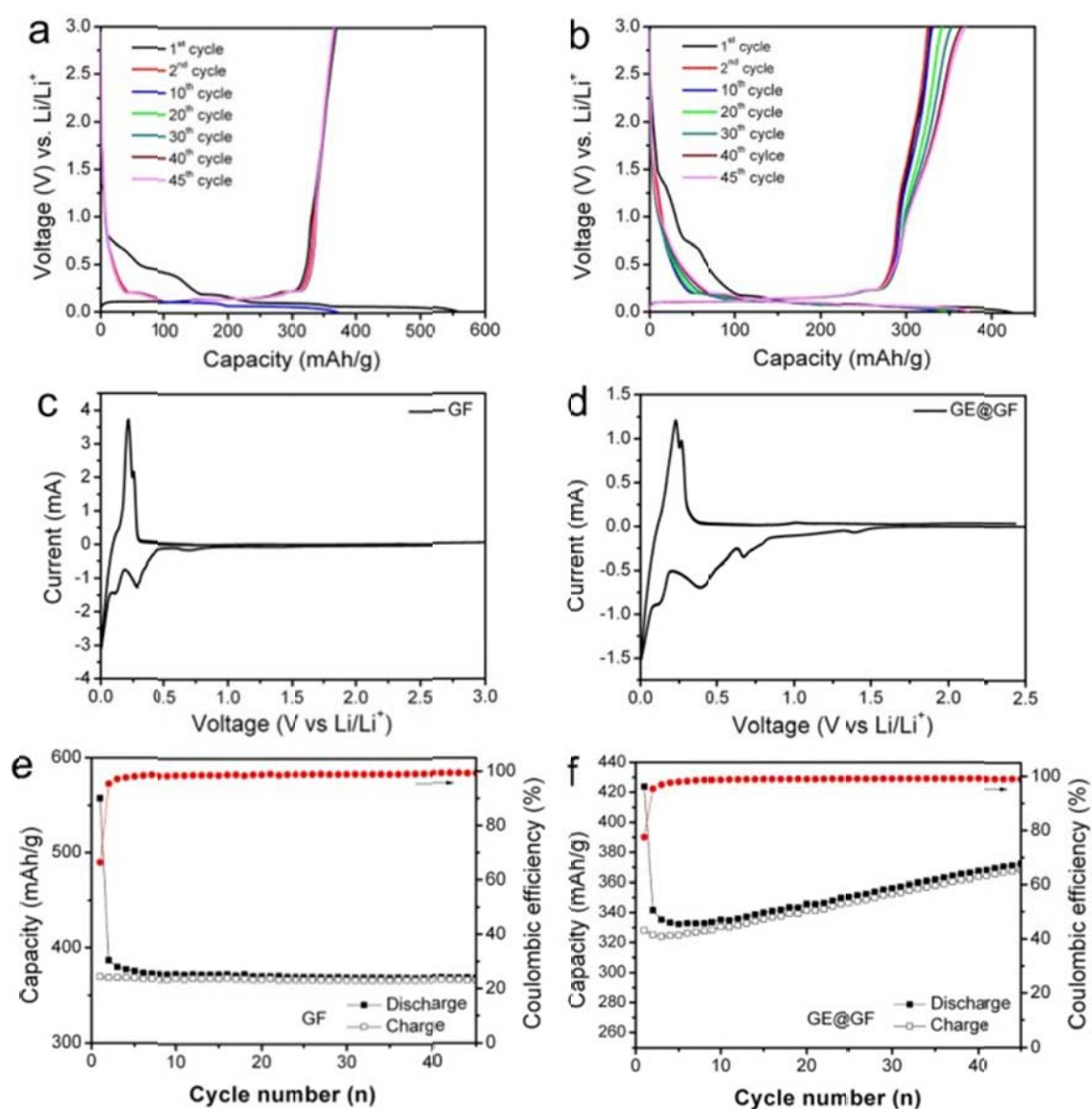


Figure 3. Electrochemical performances of GE@GF and GF. Charge/discharge profiles of (a) GF, (b) GE@GF, cyclic voltammogram of (c) GF, (d) GE@GF and cycling profile of (e) GF, (f) GE@GF. Galvanostatic cyclings were performed at current density of 37mA g^{-1} , voltage: 3.0-0.005V vs. Li/Li⁺. Cyclic voltammetry was performed at a scan rate of $58\text{ }\mu\text{s/V}$. Red plots indicate the coulombic efficiencies.

LIB with high rate capability is important industrially.³¹ The rate capabilities of these two electrodes were tested at current densities from 37 to 370 mA g^{-1} for 10 cycles each as shown in Figures 4a and 4b. The trend of decreasing capacity with higher current densities can be explained by the fact that at high current densities, the ionic motion within an electrode and/or across an electrode/electrolyte interface is not fast enough for charge distribution to reach equilibrium.³² Nonetheless, the capacity loss is recovered after reducing the rate of charge/discharge. Overall, the GE@GF electrode maintains higher capacity retention than GF electrode. In addition, GE@GF electrode demonstrates good reversibility as its capacity can be restored to $\sim 390\text{mAh g}^{-1}$ when the current density reduces to the initial value of 37 mA g^{-1} . The better rate performance of GE@GF over GF electrode can be attributed to the special structure of the egg-shell graphene. The in-filling of the graphene egg shells increases the volumetric density for Li storage and provides highly accessible thin layers for Li diffusion and intercalation. The graphene eggshell can also flex to accommodate the strain of Li⁺ intercalation.³² All these factors increase the rate of ion transfer between electrolyte and electrodes.³³

In order to further improve Li storage capacity, we nitrogen-doped the GE@GF electrode using ethylenediamine as the precursor (Details in supporting information). It has been shown previously that nitrogen- or boron-doped graphene are capable of

enhancing Li ion battery performance in terms of capacity and rate capability.^{34,35} Indeed, the storage capacity of N-doped GE@GF is enhanced. It delivers the first discharge capacity of 749 mAh g^{-1} and reversible capacity of 370 mAh g^{-1} . After 45 cycles, the capacity is increased to 459 mAh g^{-1} which is 24.5% higher than pristine GE@GF electrode (see Supporting information S4). The improved reversible capacity can be attributed to the topological defects on graphene surface caused by the N-doping, leading to a higher electronic conductivity of the active material.^{34–36} In addition, N-doped GE@GF electrode shows better rate performance (see Supporting information Figure S4) as compared to pristine graphene at all current densities. This is due to the improved electrical conductivity and electrochemical activity of doped graphene which facilitate fast charge and discharge rates.³¹

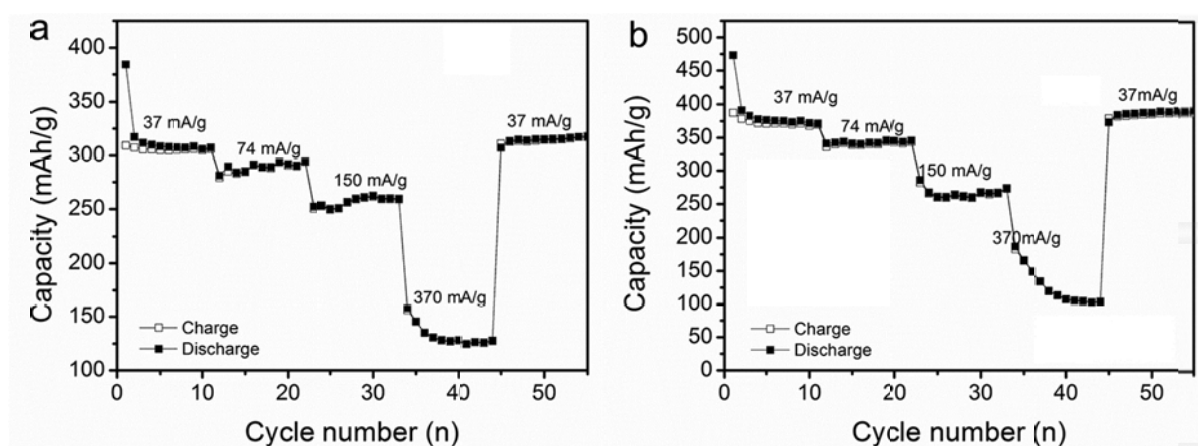


Figure 4. Rate capabilities of (a) GF and (b) GE@GF electrodes over a range of current densities (37 to 370 mA g^{-1}).

To obtain further insight into the Li intercalation mechanism of GE@GF electrode, we employed in-situ Raman spectroscopy to follow the lithiation process. Figure 5 shows 3-dimensional *in-situ* Raman spectra collected during discharging process of

the GE@GF electrode. Overall, it can be observed that G-band shifts gradually to higher wavenumber and its intensities decrease when it is polarized from 3.0V to 0.005V *vs.* Li/Li⁺. The upshift of G-band indicates the doping effect on graphene where electrons transfer from Li to graphene during intercalation.³⁷ As evidenced by Figure 5b, G-band intensities weaken upon further polarization and finally disappears at 0.14V. The disappearance of G-band signifies that Li doping level has reached its maximum level on GE@GF electrode, which causes a reduction in optical skin depth and Raman scattering intensity.³⁸ This indicates that stage-1 LiC₆ phase has formed on the lithiated GE@GF electrode. This observation agrees with previous finding reported by Pollak *et al.*³⁷ and is also verified by our experiments on commercial graphite (See Supporting Information Figure S5)

We also performed *ex-situ* ⁷Li Nuclear Magnetic Resonance (NMR) for GE@GF electrode which was fully discharged to 0.005V. The NMR spectrum shows the appearance of a peak at 42 ppm which suggests Li can intercalate into graphene layers of GE@GF electrodes to form stage-1 LiC₆ (Figure S6). This is in good agreement with the observation in graphite electrode as reported by Trease *et al.*³⁹

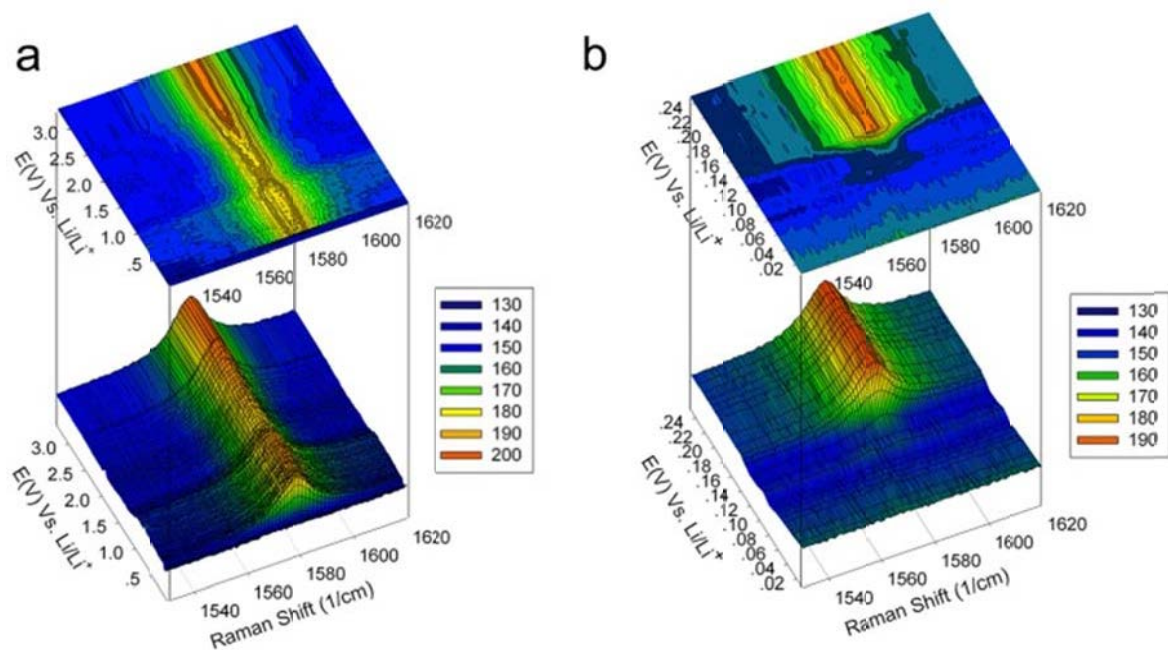


Figure 5. (a) *In-situ* Raman spectra of GE@GF electrode discharged from 3.0V to 0.005V vs. Li/Li^+ . (b) Showing details of (a) at the range from 0.25V to 0.005V vs. Li/Li^+ .

CONCLUSIONS

In conclusion, we have demonstrated a method to improve the capacity of microporous graphene electrodes by in-filling its cavities with graphene eggshells. The eggshell increases the volumetric energy density and its interconnected networks shorten the Li-ion diffusion pathway and ultimately enhance the rate capabilities. Such morphology control is also effective in improving the initial coulombic efficiency of the unfilled graphene foam by 17%. Mechanistic study using *in-situ* Raman and *ex-situ* NMR reveals that the Li intercalation mechanism of GE@GF electrode resembles that of bulk graphite, that is, *via* stage Li-graphite intercalated compounds, although its overall capacity is higher than that of the theoretical values of graphite. Further work on improving reversible capacity is under way.

List of Publications and Significant Collaborations that resulted from your AOARD supported project:

Filling the Voids of Graphene Foam with Graphene Eggshell for Improved Lithium-Ion Storage, Bee-Min Goh^{†,#}, Yu Wang^{†,#}, M.V. Reddy[†], Yuan Li Ding[§], Li Lu[§], Christopher Bunker[‡] and Kian Ping Loh^{†,*}
***ACS Applied Materials*, DOI: 10.1021/am5022655**